Center of mass velocity-based predictions in balance recovery following pelvis perturbations during human walking

Vlutters, M; van Asseldonk, EHF; van der Kooij, Herman

DOI
10.1242/jeb.129338

Publication date
2016

Document Version
Final published version

Published in
The Journal of Experimental Biology

© 2016. Published by The Company of Biologists Ltd | Journal of Experimental Biology (2016) 219, 1514-1523 doi:10.1242/jeb.129338

RESEARCH ARTICLE

Center of mass velocity-based predictions in balance recovery following pelvis perturbations during human walking

M. Vlutters[1,*], E. H. F. van Asseldonk[1] and H. van der Kooij[1,2]

ABSTRACT

In many simple walking models, foot placement dictates the center of pressure location and ground reaction force components, whereas humans can modulate these aspects after foot contact. Because of the differences, it is unclear to what extent predictions made by models are valid for human walking. Yet, both model simulations and human experimental data have previously indicated that the center of mass (COM) velocity plays an important role in regulating stable walking. Here, perturbed human walking was studied to determine the relationship of the horizontal COM velocity at heel strike and toe-off with the foot placement location relative to the COM, the forthcoming center of pressure location relative to the COM, and the ground reaction forces. Ten healthy subjects received mediolateral and anteroposterior pelvis perturbations of various magnitudes at toe-off, during 0.63 and 1.25 m s^{-1} treadmill walking. At heel strike after the perturbation, recovery from mediolateral perturbations involved mediolateral foot placement adjustments proportional to the mediolateral COM velocity. In contrast, for anteroposterior perturbations, no significant anteroposterior foot placement adjustment occurred at this heel strike. However, in both directions the COM velocity at heel strike related linearly to the center of pressure location at the subsequent toe-off. This relationship was affected by the walking speed and was, for the slow speed, in line with a COM velocity-based control strategy previously applied by others in a linear inverted pendulum model. Finally, changes in gait phase durations suggest that the timing of actions could play an important role during the perturbation recovery.

KEY WORDS: Human balance, Perturbed walking, Foot placement, Extrapolated center of mass, Capture point

INTRODUCTION

Humans are currently unparalleled when it comes to bipedal walking. Despite a relative high located center of mass (COM) and small base of support (BoS), movement can be maintained or altered at will. Various strategies such as adjustments to the location and timing of foot placement, and adjustments to ankle and hip torques can be addressed to control balance during unconstrained walking. These strategies affect the magnitude, direction and point of application of the ground reaction force, with the point of application being the center of pressure (COP). The force components affect the COM acceleration. Together with the COP location relative to the COM, they also determine the angular acceleration of the whole body about the COM. Predicting how healthy humans shift the COP and modulate the ground reaction force could aid in fall prevention in humans, exoskeletons and bipedal robots, as faulty weight shifting could easily lead to a fall (Robinovitch et al., 2013).

Simple models such as the inverted pendulum have been extensively used to describe human locomotion (Townsend, 1985; Kajita and Tani, 1991; Winter, 1995; Garcia et al., 1998; Kuo, 2001). These models incorporate foot placement, which is considered a major strategy in directing locomotion in both mediolateral (ML) and anteroposterior (AP) movement directions (MacKinnon and Winter, 1993; Patla, 2003). However, these models do not capture several other important aspects of walking (see Fig. 1A). First, the double support phase is often neglected. Consequently, the COM does not move between heel strike and toe-off. Second, the area of the foot is often infinitesimal, such that foot placement fully determines the COP location during single support. Third, if no inertia properties are present in the model, the ground reaction force will always pass exactly through the COM. This way, foot placement also fully determines the ground reaction force components. In humans, the COP makes a continuous shift from the trailing foot at heel strike to the leading foot at toe-off (Jian et al., 1993), during which the COM continues to move. Furthermore, humans have mechanisms other than foot placement to alter the COP location and ground reaction force. Hence, many inverted pendulum models might not correctly represent the spatio-temporal location of the COP as well as the ground reaction forces following foot placement.

Despite the differences, both model simulations and data collected in humans suggest an important role of the COM velocity in regulating stable walking. The horizontal position and velocity of the COM have predictive properties in human foot placement. Using the pelvis as an approximation of the COM, a linear function of the ML pelvis position and velocity relative to the stance foot at mid-stance could be used to predict over 80% of the variance in ML foot placement during unperturbed human treadmill walking (Wang and Srinivasan, 2014). Pelvis predictive power was lower for AP foot placement, explaining just over 30% at mid-stance. In a 3D spring-loaded inverted pendulum model, stable running (Peuker et al., 2012) and walking (Maus and Seyfarth, 2014) could be realized by setting the swing leg angle of attack proportional to the angle of the COM velocity vector with the vertical. Both studies reported that this leads to increased stability compared with strategies that did not take into account COM velocity. In a planar bipedal robot, stable running could be achieved by setting the swing leg angle of attack proportional to the horizontal COM velocity (Hodgins and Raibert, 1991). Foot placement strategies directly proportional to the horizontal COM velocity were also derived from a linear inverted pendulum model's energy orbits, which allowed a low-dimensional robot to walk for several steps (Kajita et al., 1992).

[1]Department of Biomechanical Engineering, University of Twente, Enschede, Horstring W215, 7500 AE, The Netherlands. [2]Department of Biomechanical Engineering, Delft University of Technology, Delft 2628 CD, The Netherlands.

*Author for correspondence (m.vlutters@utwente.nl)

Received 30 July 2015; Accepted 2 March 2016

Journal of Experimental Biology

Journal of Experimental Biology (2016) 219, 1514-1523 doi:10.1242/jeb.129338

List of symbols and abbreviations

AP	anteroposterior
BoS	base of support
COM	center of mass
COP	center of pressure
g	Earth's gravitational constant (9.81 m s^{-2})
HSR	heel strike right
l	leg length
l_0	length scaling value (Euclidean distance between the COM of the feet at HSR)
ML	mediolateral
R_D	ratio of the horizontal distance COP–COM and the vertical COM height (in either ML or AP direction)
R_F	ratio of the horizontal and the vertical ground reaction force components (in either ML or AP direction)
TOL	toe-off left
TOR	toe-off right
XCOM	extrapolated center of mass
ω_0^{-1}	XCOM proportionality constant

A special case of these energy orbits (zero energy) can be used to obtain the extrapolated center of mass (XCOM) (Hof et al., 2005) or capture point (Pratt et al., 2006). This concept can be conceived as a point on the floor at a horizontal distance from the COM that is directly proportional to the horizontal COM velocity (see Fig. 1B). The proportionality constant is $\omega_0^{-1} = \sqrt{(l/g)}$, in which g is the Earth's gravitational constant and l is the pendulum (leg) length. It is the reciprocal of the eigenfrequency of a linear inverted pendulum model. This model can come to an upright stop by placing the COP in the XCOM. In simulations, stable walking could be achieved by placing the COP at a fixed offset from the XCOM in both the ML and AP directions, using a fixed step time (Hof, 2008). This 'constant offset control' allowed the model to return to a stable gait after perturbing the COP location at heel strike. This concept is supported by experimental data, suggesting that humans also apply ML constant offset control in both normal (Hof et al., 2007) and ML perturbed walking (Hof et al., 2010). In the former work, it was concluded that foot placement is the primary strategy for realizing the ML COP offset, and that an ankle torque allows minor COP adjustments through feedback after the foot has been placed. This also means that the offset can be realized in ways other than foot placement alone, not captured by the linear inverted pendulum model from which the XCOM concept is derived. This is especially the case in the AP direction, not investigated in Hof's work, where COP shifts are most feasible because of the dimensions of the foot.

Simple walking models and the concepts derived from them can give insight into human balance control, but might also fail to accurately describe human balance during walking because of their simplicity. In many inverted pendulum models, foot placement is directly linked to the COP location and the ground reaction force components. As these concepts are not strictly linked in humans, it is unclear to what extent predictions made by these models are valid for human walking. Yet, both model simulations and human experimental data suggest some proportionality of one or more of these concepts with the COM velocity. In this study, we investigate relationships between the horizontal COM velocity and (1) the location of the foot relative to the COM, (2) the location of the COP relative to the COM and (3) the ground reaction force components. Only the instances of the first heel strike and toe-off following ML and AP perturbations are chosen for analysis. These are often a single key instance in inverted pendulum models, at which the model state determines subsequent ballistic motion. Variables 2 and 3 will only be investigated at toe-off, because these are not influenced yet by foot placement at the instance of heel strike.

MATERIALS AND METHODS

Participants

Ten healthy volunteers with no known history of neurological, muscular or orthopedic problems participated in the study (five men, age 25±2 yr, weight 67±12 kg, height 1.80±0.11 m, means±s.d.). The setup and experimental protocol were approved by the local ethics committee. All subjects gave prior written informed consent in accordance with the Declaration of Helsinki.

Apparatus

Subjects walked on a dual-belt instrumented treadmill (custom Y-Mill, Motekforce Link, Culemborg, The Netherlands). A force plate beneath each belt was used to measure 3 degrees-of-freedom ground reaction forces and moments. To perturb subjects in both ML and AP directions, two motors (SMH60, Moog, Nieuw-Vennep, The Netherlands) were located adjacent to the treadmill, one to the right and one at the rear. The motors were bolted onto a steel support

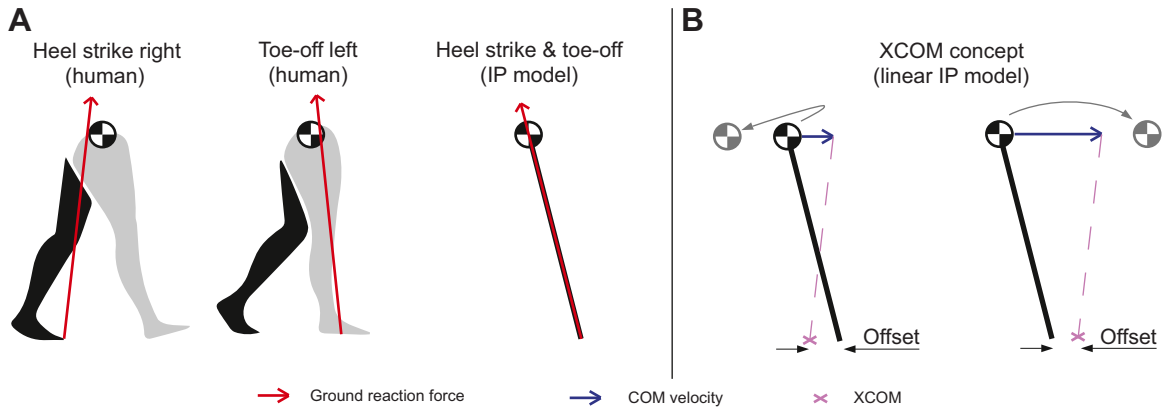

Fig. 1. Schematic overview of concepts in human and inverted pendulum (IP) model walking. (A) At heel strike, the center of pressure (COP) is near the trailing foot in humans. It takes until the subsequent toe-off for it to fully shift to the leading leg. In many inverted pendulum models, the instances of heel strike and toe-off coincide, and so do the foot and COP locations. Furthermore, the ground reaction force often passes exactly through the COM in these models. (B) The extrapolated center of mass (XCOM) is a concept derived from a linearized inverted pendulum model, which can be considered as a point on the floor at a distance from the COM that is directly proportional to the COM velocity. Moving the COP beyond the XCOM makes the pendulum fall back in the direction from which it came. Moving the COP before the XCOM makes the pendulum topple over the COP. Placing the COP exactly in the XCOM brings the pendulum to an upright stop.

Journal of Experimental Biology (2016) 219, 1514-1523 doi:10.1242/jeb.129338

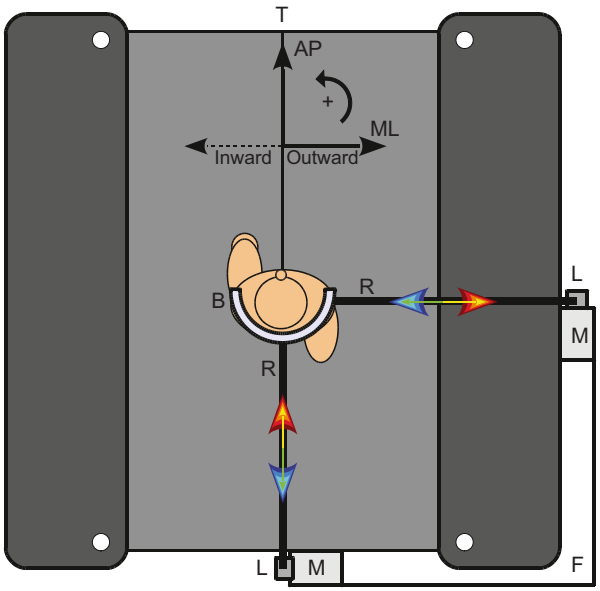

Fig. 2. Schematic overview of the perturbation setup. Two motors adjacent to a dual belt instrumented treadmill can be used to perturb the subject at the pelvis during walking. Colored arrows indicate the direction of the different perturbation magnitudes of 0.04, 0.08, 0.12 and 0.16 times body weight (positive: yellow–red, negative: green–blue). An inward perturbation is regarded as a perturbation toward the (left) stance leg, an outward perturbation away from the stance leg. B, pelvis brace; F, support frame; L, lever arms; M, motors; R, rods; T, dual belt instrumented treadmill.

structure that was tightly clamped to the exterior frame of the treadmill, without influencing the force plates. Each motor had an aluminum lever arm (0.3 m) attached to its rotational axis, onto which a load cell (model QLA131, FUTEK, Los Angeles, CA, USA) was located for torque sensing. A ball joint was located at the end of each lever arm, to which an aluminum rod (0.8 m in length, 0.3 kg) could be attached. The other end of each rod could be attached to the right or rear of a modified universal hip abduction brace (Distrac Wellcare, Hoegaarden, Belgium), also using a ball joint. The brace (0.9 kg) could be tightly worn around the pelvis by the subject. With the lever arms in neutral position (vertical), the ball joints of the lever arm were 1 m above the walking surface of the treadmill, such that the rods were approximately horizontal when the brace was worn by a subject. The maximum possible excursion of each motor was 1.1 rad in each direction of the neutral position, allowing up to 0.55 m pelvis excursion. A schematic overview of the setup is shown in Fig. 2. Motor control signals were generated at 1000 Hz using xPC-target (MathWorks, Natick, MA, USA) and sent to the motor drivers over ethernet (User Datagram Protocol), using a dedicated ethernet card (82558 ethernet card, Intel, Santa Clara, CA, USA).

Data collection

Motor torque and encoder angle were collected at 1000 Hz using the ethernet card. Kinematic data were acquired using a 12-camera motion capture system (Visualeyez II, Phoenix Technologies, Burnaby, Canada). In total, nine three-LED marker frames were placed on the subject. Frame locations were on the feet, lower legs, upper legs, the front of the pelvis below the strap of the brace, the sternum and the head. Additional single LEDs were placed on the lateral epicondyles of the femur and on the lateral malleoli. Ground reaction force data were captured at 1000 Hz using a PCI-6229 AD card (National Instruments, Austin, TX, USA), also using xPC-target software. The same card was used to generate an analog signal for synchronization with the motion capture system.

Protocol

Prior to the experiment, several kinematic measurements were taken during which bony landmarks were indicated using an LED-based probe, as described in Cappozzo et al. (1995). Captured landmarks were the calcaneus, first and fifth metatarsal heads, medial and lateral malleoli, fibula head, medial and lateral epicondyles of the femur, greater trochanter, anterior and posterior superior iliac spines, xiphoid process, jugular notch, seventh cervical vertebra, occiput, head vertex and nasal sellion (Dumas et al., 2007).

During the experiment, subjects were instructed to walk on the treadmill with their arms crossed over the abdomen. A safety harness was worn to prevent injury in case of a fall. The brace was tightly worn around the pelvis. Subjects walked four blocks of three trials each. The first trial of each block was a 2 min unperturbed walking trial, the second and third were perturbation trials. In two blocks, subjects were attached to the right motor, and in the other two blocks to the rear motor. Subjects were never attached to both motors simultaneously to minimize restraints. The attachment order was randomized. For each motor attachment site, subjects walked one block at a slow speed ($0.63 \times \sqrt{l}\,\mathrm{m\,s^{-1}}$) and one at a normal speed ($125 \times \sqrt{l}\,\mathrm{m\,s^{-1}}$, where $\sqrt{l}$ is the square root of the subject's leg length; Hof, 1996). Subjects walked the slow trials first, followed by the normal trials for the same motor. In addition to the mandatory rest after two blocks, subjects were free to take breaks between trials.

During perturbation trials subjects randomly received perturbations at toe-off right (TOR), detected using the vertical ground reaction force (threshold 5% body weight). Toe-off was chosen for perturbation onset to maximally allow foot placement adjustment, while preventing push-off modulation in response to the disturbance. A random interval of approximately 6–12 s was given between perturbations. Perturbation signals consisted of 150 ms block pulses resulting in force magnitudes equal to 4, 8, 12 and 16% of the subject's body weight. Perturbation force direction was either inward (negative sign, leftward for right swing leg) and outward (positive sign, rightward for right swing leg) or backward (negative sign) and forward (positive sign), depending on the motor in use (see Fig. 2). Each condition was repeated eight times, giving 256 perturbations in total (32 per trial). All perturbations were randomized over magnitude and direction within each block. When no perturbation was being applied, the motors were admittance controlled, actively regulating the interaction force between subject and motor to (near) zero.

Data processing

All data were processed using MATLAB (R2014b, MathWorks). Raw perturbation forces were integrated to obtain the impulse delivered by the motors. Ground reaction force and moment data were filtered with a fourth-order 40 Hz zero-phase Butterworth filter before calculating a COP location. Marker data were filtered with a fourth-order 20 Hz zero phase Butterworth filter. Local landmark positions (relative to their respective marker frames) were extracted from the probe measurements. In each trial, the global landmark positions were reconstructed using least squares estimation of a rotation matrix and a displacement vector between the local and global marker frame coordinates (Söderkvist and Wedin, 1993).

Landmark data of the feet were used to detect the gait phase, comparable to Zeni et al. (2008). The maximum backward excursion of the metatarsal head I was used to detect toe-off. Heel strike was detected as the instance at which the AP calcaneus

Journal of Experimental Biology (2016) 219, 1514-1523 doi:10.1242/jeb.129338

velocity stopped decreasing following its largest forward excursion. Furthermore, landmarks were used to estimate the locations of the ankle, knee, hip, lumbar and cervical joints, as well as the COM locations of the feet, lower legs, upper legs, pelvis, torso and head (Dumas et al., 2007). The available segment COM locations were used to calculate a weighted total COM location.

Unperturbed walking data were used as baseline for the trials with a corresponding walking speed. All data were made dimensionless according to Hof (1996). For each subject, the baseline average Euclidean distance between the COM of the feet at heel strike was used as the length scaling value (l_0). Subject mass was used to scale forces. Perturbation onsets were identified from the motor reference signals. All perturbation data were cut into sequences from 0.5 s before to 2.5 s after perturbation onset, and were sorted by perturbation type and walking speed. All position and velocity data were expressed relative to those of the COM. The velocity of the COM itself was expressed relative to the walking surface by adding the belt speed to the AP COM velocity.

For each subject, the ML and AP ground reaction forces were divided by the vertical ground reaction force to find the force ratio R_F in the ML and AP directions, respectively. For comparison, the ML and AP distances between the COP and the COM were divided by the COM height to find the distance ratio R_D in the ML and AP directions, respectively. For each subject, position, velocity, force and ratio data were averaged over the repetitions at the instances of the first heel strike right (HSR) and toe-off left (TOL) after perturbation onset. Furthermore, the durations between perturbation onset at TOR and HSR, as well as that between HSR and the subsequent TOL, were determined and averaged over the repetitions within each subject. Finally, repetition averages of each subject were used to calculate subject averages and standard deviations.

Linear least squares fits of the form $y=ax+b$ were made to the subject average data. The independent variable x was the ML or AP COM velocity at HSR or TOL. The dependent variable y was one of the following: the distance between the COM and the COM of the leading foot; the distance between the COM and the COP; a horizontal ground reaction force component; ratio R_F; or ratio R_D (each in the ML or AP direction at HSR or TOL). For comparison, a dimensionless XCOM proportionality constant (ω_0^{-1}) was calculated for each subject. These were subsequently used to find a subject average proportionality constant and a subject average ML or AP XCOM=$\omega_0^{-1}\times x$, where the XCOM is relative to the COM, and x corresponds to the horizontal ML or AP COM velocity at any given instance.

Linear mixed models were used to assess the effects of the perturbation (fixed factor, with intercept) and walking speed (fixed factor, with intercept) on the distance between the COM and the COM of both feet at HSR and TOL, the distance between the COM and the COP at TOL, the ground reaction force components at TOL, as well as the duration of the single and double support phase following the perturbation. Subject effects were included as a random factor (intercept) to account for the correlation between repeated measurements within a single subject. A significance level of α=0.050 was used and a Bonferroni correction was applied to correct for multiple comparisons during *post hoc* analysis. In the latter, the perturbed conditions were only compared with the unperturbed walking condition and not mutually. SPSS statistics 21 (IBM Corporation, Armonk, NY, USA) was used for the statistical analysis.

RESULTS

Subject balance responses were assessed following ML and AP perturbations during both slow and normal walking. Here results will only be visualized for the slow walking speed. The normal walking speed yielded mostly comparable results (see Figs S1–S3). Statistical values apply to both slow and normal walking speeds unless indicated otherwise. Subject average data are shown dimensionless. Subject average scaling values for the slow walking speed are l_0=0.44±0.04 m for distances, $\sqrt{(g \times l_0)}=2.08\pm0.10$ m s^{-1} for velocities and $\sqrt{(l_0/g)}=0.21\pm0.01$ s for durations, where l_0 is the average Euclidean distance between the COM of the feet at heel strike during unperturbed walking. For the normal walking speed, scaling values are l_0=0.63±0.06 m, $\sqrt{(g \times l_0)}=2.48\pm0.11$ m s^{-1} and $\sqrt{(l_0/g)}=0.25\pm0.01$ s.

Perturbations

Perturbations of various magnitudes (±0.04, ±0.08, ±0.12, ±0.16×body weight) were applied to the subject's pelvis at TOR using two admittance-controlled motors. Although the motors

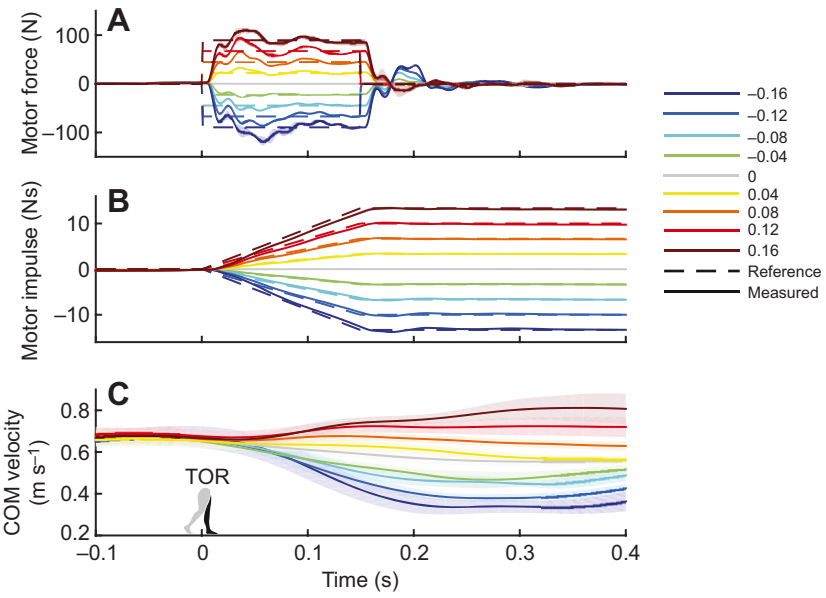

Fig. 3. Typical single-subject anteroposterior (AP) perturbation profile. (A) Reference (dashed) and measured (solid) motor force. (B) Reference (dashed) and measured (solid) motor impulse, obtained by integrating the motor forces. (C) AP COM velocity relative to the walking surface. Colors indicate the various perturbation magnitudes as a ratio of body weight. Lines are within-subject means for a single subject. Shaded areas indicate the within-subject standard deviation.

Journal of Experimental Biology (2016) 219, 1514-1523 doi:10.1242/jeb.129338

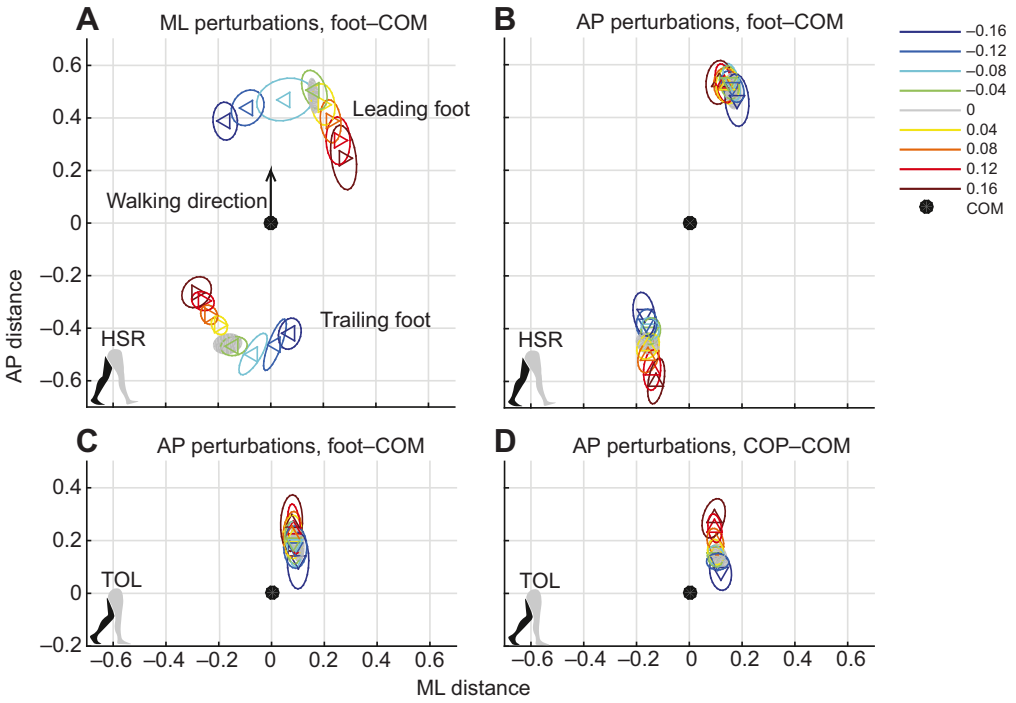

Fig. 4. Positions of the COM of the feet and the COP relative to the COM. (A) At heel strike right (HSR), the location of the COM of the leading and trailing foot relative to the COM in (0,0), for ML perturbations. (B) Same as A, but for AP perturbations. (C) At toe-off left (TOL), location of the COM of the leading foot relative to the COM for AP perturbations. (D) At TOL, location of the COP relative to the COM for AP perturbations. Triangles show subject means and indicate the perturbation direction. Ellipses represent the subject standard deviation. Colors indicate the various perturbation magnitudes. Data shown are dimensionless and for slow walking only.

cannot exactly track the reference block pulses, the integrals of the reference and measured perturbation force are similar. Effects of the different perturbations on the horizontal COM velocity can be clearly distinguished (see Fig. 3).

Balance responses

Various balance responses were observed to recover from the perturbation (see Fig. 4). At HSR, the leading foot was placed further inward (leftward for right swing leg) or outward (rightward for right swing leg) with increasing inward (ML, negative sign) or outward (ML, positive sign) perturbation magnitude, respectively. The ML distance between the COM and the leading foot was significantly affected by the ML perturbation magnitude ($F_{8,153}$=363.005, P<0.001), walking speed ($F_{1,153}$=71.916, P<0.001) and their interaction ($F_{8,153}$=9.300, P<0.001). For slow walking, the distance between the COM and the leading foot was significantly different from that in unperturbed walking for all but the lowest magnitude perturbations (P≤0.001). For the normal speed, this was the case for all but the lowest magnitude outward perturbations (P≤0.025).

At TOL, the ML distance between the COM and the leading foot was decreased compared with that at HSR, but was still significantly affected by ML perturbation magnitude ($F_{8,153}$=351.252, P<0.001), speed ($F_{1,153}$=15.283, P<0.001) and their interaction ($F_{8,153}$=3.899, P<0.001). This distance was significantly different from that in unperturbed walking for all but the lowest inward perturbation magnitudes for both slow (P≤0.033) and normal (P≤0.009) walking speeds. The ML distance between the COM and the COP showed similar effects of ML perturbation magnitude ($F_{8,153}$=399.611, P<0.001), speed ($F_{1,153}$=20.970, P<0.001) and their interaction ($F_{8,153}$=5.225, P<0.001). This distance was significantly different from that in unperturbed walking for all but the lowest magnitude inward perturbations, for both slow (P≤0.006) and normal (P≤0.002) walking speeds.

The ML ground reaction force at TOL also changed significantly with perturbation magnitude ($F_{8,153}$=489.051, P<0.001), speed ($F_{1,153}$=9.849, P=0.002) and their interaction ($F_{8,153}$=26.742, P<0.001). With the exception of the lowest magnitude perturbations for slow walking, all ML perturbations led to ML forces at TOL significantly different from that in unperturbed walking (slow: P≤0.001, normal: P≤0.043). Although the vertical force at TOL was also significantly affected by ML perturbation magnitude ($F_{8,153}$=10.506, P<0.001), speed ($F_{1,153}$=401.749, P<0.001) and their interaction ($F_{8,153}$=3.440, P=0.001), it was not significantly different from the vertical force in unperturbed walking for any ML perturbation during slow walking (P≥0.209). For the normal walking speed it was significantly different for the larger (−0.12, ±0.16) perturbation magnitudes (P≤0.002).

For AP perturbations, subjects barely adjusted the AP distance between the COM and the leading foot at HSR. Although this distance was significantly affected by the AP perturbation magnitude ($F_{8,153}$=2.650, P=0.009), speed ($F_{1,153}$=50.985, P<0.001) and their interaction ($F_{8,153}$=5.094, P<0.001), it was not significantly different from that in unperturbed walking for any AP perturbation for either slow (P≥0.124) or normal (P≥0.324) walking speeds. The AP distance between the COM and the trailing foot was also significantly affected by AP perturbation magnitude ($F_{8,153}$=65.671, P<0.001), speed ($F_{1,153}$=86.310, P<0.001) and their interaction ($F_{8,153}$=4.658, P<0.001). For slow walking, this distance was significantly different from that in unperturbed walking following all but the lowest magnitude AP perturbations (P≤0.017). For the normal walking speed, it was different for the larger magnitude (+0.12, ±0.16) AP perturbations (P<0.013).

At TOL, the AP distance between the COM and the leading foot showed more of an effect of the AP perturbation magnitude than at HSR. This distance at TOL was significantly affected by AP perturbation magnitude ($F_{8,153}$=20.149, P<0.001) and speed ($F_{1,153}$=139.137, P<0.001), but not by their interaction ($F_{8,153}$=1.563, P=0.140). This distance was significantly different from that in unperturbed walking for the larger magnitude (0.08, 0.12 and 0.16) forward and −0.16 backward perturbations

Journal of Experimental Biology

Journal of Experimental Biology (2016) 219, 1514-1523 doi:10.1242/jeb.129338

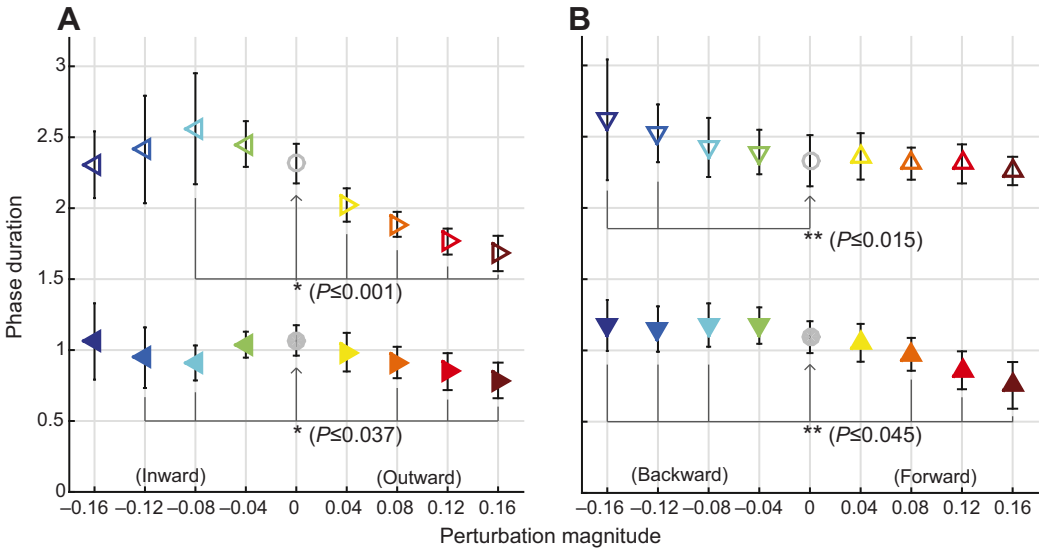

Fig. 5. Gait phase duration following perturbations. Gait phase duration directly following (A) ML and (B) AP perturbations. Single and double support phase durations are indicated by the open and filled symbols, respectively. Triangles show subject averages and indicate the perturbation direction. Error bars indicate the subject standard deviation. Colors indicate the various perturbation magnitudes. Asterisks (*) indicate significant differences from the corresponding unperturbed phase duration. Double asterisks (**) indicate that there was no significant interaction effect between slow and normal walking, such that the corresponding *P*-values represent both slow and normal walking speeds. Data shown are dimensionless and for slow walking only.

($P \leq 0.030$). The AP distance between the COM and the COP at TOL shows more variation in the means than the AP distance between the COM and the leading foot at TOL. This distance between COM and COP was significantly affected by AP perturbation magnitude ($F_{8,153}=65.583$, $P<0.001$), speed ($F_{1,153}=64.175$, $P<0.001$) and their interaction ($F_{8,153}=3.517$, $P=0.001$). For slow walking, this distance was significantly different from that in unperturbed walking for the larger magnitude (0.08, 0.12 and 0.16) forward and −0.16 backward perturbation ($P \leq 0.001$). This is similar for the normal walking speed, which also showed a significant difference for the −0.12 backward perturbation ($P \leq 0.013$).

Subjects adjusted the AP ground reaction force at TOL significantly with AP perturbation magnitude ($F_{8,153}=122.686$, $P<0.001$), speed ($F_{1,153}=677.983$, $P<0.001$) and their interaction ($F_{8,153}=11.086$, $P<0.001$). For slow walking, AP forces were significantly different from that in unperturbed walking for the larger magnitude (0.08, 0.12 and 0.16) forward and −0.16 backward perturbations ($P \leq 0.011$). For the normal walking speed, all AP perturbations led to significant differences ($P \leq 0.043$). The vertical force component was significantly affected by AP perturbation magnitude ($F_{8,153}=79.415$, $P<0.001$), speed ($F_{1,153}=583.701$, $P<0.001$) and their interaction ($F_{8,153}=32.201$, $P<0.001$). However, with the exception of the largest forward perturbation magnitude, none of the AP perturbations led to vertical forces significantly different from that in unperturbed slow walking ($P \geq 0.875$). In contrast, for the normal speed, all but the smallest forward perturbation led to significant differences ($P \leq 0.019$).

Finally, both the ML and AP perturbations had a significant effect on the single support duration during which the perturbation was applied (ML: $F_{8,153}=47.370$, $P<0.001$, AP: $F_{8,153}=7.581$, $P<0.001$), as well as on the following double support duration (ML: $F_{8,153}=8.941$, $P<0.001$, AP: $F_{8,153}=51.762$, $P<0.001$). Walking speed also significantly affected these single (ML: $F_{1,153}=715.091$, $P<0.001$, AP: $F_{1,153}=1354.447$, $P<0.001$) and double support durations (ML: $F_{1,153}=1313.883$, $P<0.001$, AP: $F_{1,153}=2073.293$). Interaction effects of perturbation magnitude and walking speed only occurred for ML perturbations in both single ($F_{8,153}=12.833$, $P<0.001$) and double support durations ($F_{8,153}=4.412$, $P<0.001$). Durations significantly different from that in unperturbed walking and the corresponding *P*-values can be found in Fig. 5 and Fig. S1 for slow and normal walking, respectively.

Relationships with COM velocity

The relationship between the horizontal COM velocity and (1) the location of the foot relative to the COM, (2) the location of the COP relative to the COM and (3) the ground reaction force components were investigated at the instances of the first HSR and TOL following perturbation onset at TOR. Combinations of instances (HSR, TOL) were also investigated, analogous to walking models without a double support phase. The coefficients of determination (R^2) of the linear least squares fits made to these data are shown in

Table 1. Coefficients of determination (R^2) of the linear least squares fits made to the data for slow and normal walking speeds

	COM velocity at HSR		COM velocity at TOL	
	Slow	Normal	Slow	Normal
Mediolateral				
Foot–COM distance at HSR	0.983	0.996	0.986	0.978
Foot–COM distance at TOL	0.989	0.996	0.966	0.968
COP–COM distance at TOL	0.993	0.997	0.964	0.968
Ground reaction force at TOL	0.998	0.998	0.957	0.968
R_F at TOL	0.997	0.996	0.955	0.968
R_D at TOL	0.994	0.997	0.964	0.967
Anteroposterior				
Foot–COM distance at HSR	0.281	0.917	0.069	0.941
Foot–COM distance at TOL	0.851	0.916	0.426	0.847
COP–COM distance at TOL	0.982	0.974	0.672	0.920
Ground reaction force at TOL	0.988	0.992	0.696	0.963
R_F at TOL	0.983	0.973	0.668	0.923
R_D at TOL	0.984	0.973	0.681	0.916

Underlined values correspond with a fit of which the root mean square error is less than 5% of the range of the dependent variable. COM, center of mass; COP, center of pressure; HSR, heel strike right; R_D, distance ratio; R_F, force ratio; TOL, toe-off left.

Journal of Experimental Biology (2016) 219, 1514-1523 doi:10.1242/jeb.129338

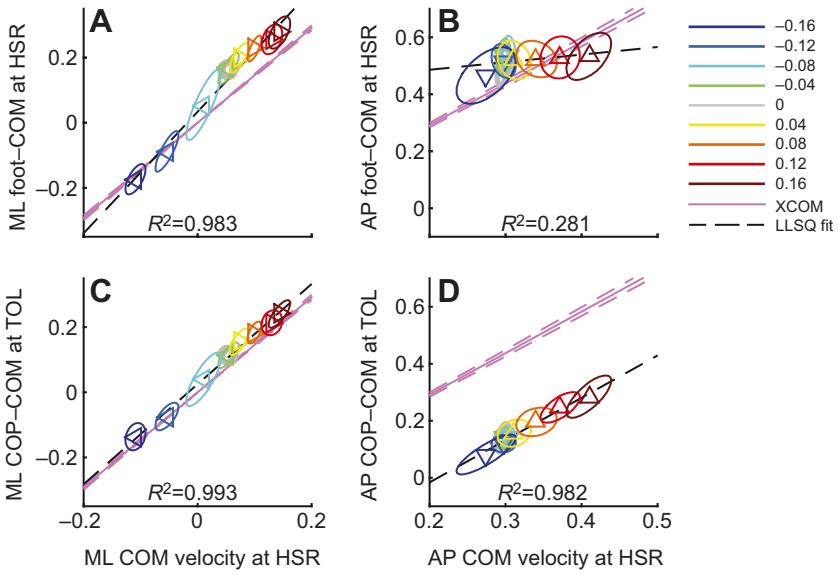

Fig. 6. Various relationships between COM velocity and both the leading foot and COP. (A) ML COM velocity at HSR versus ML distance between the COM and the leading foot at HSR, for ML perturbations. (B) Same as A, but in the AP direction for AP perturbations. (C) ML COM velocity at HSR versus ML distance between the COM and COP at TOL for ML perturbations. (D) Same as C, but in the AP direction for AP perturbations. Triangles show subject means and indicate the perturbation direction. Ellipses represent the subject standard deviation. Colors indicate the various perturbation magnitudes. Pink solid and dashed lines indicate the subject mean and standard deviation, respectively, of the XCOM relative to the COM. This XCOM line has slope ω_0^{-1} and no intercept. The black dashed line is a linear least squares (LLSQ) fit to the data. R^2 indicates the coefficient of determination of the fit. Data shown are dimensionless and for slow walking only.

Table 1. Results for the COP, forces, R_F and R_D at HSR were omitted, as these are not yet affected by foot placement at this instance. For several fits, corresponding data are shown in Figs 6 and 7 for slow walking, and in Figs S2 and S3 for normal walking speed.

For ML perturbations, the ML distance between the COM and the leading foot changed directly proportional with the ML COM velocity at HSR. Similar effects can be observed for the ML distance between the COM and the COP (see Fig. 6, Fig. S2). At TOL, there are only minor differences in the ML distance between the COM and the leading foot, and between the COM and the COP. This gives rise to approximately the same linear relationships. For distances in the ML direction, the strongest linear relationships were found between the COM velocity at HSR and the distance between the COM and the COP at TOL. For slow walking, the slope of the fit to this data (y=1.54x+0.03, R^2=0.993) corresponds well with the subject average dimensionless ω_0^{-1} (1.46±0.04). For the normal speed, this slope (y=1.48x+0.04, R^2=0.99) shows more deviation from the corresponding ω_0^{-1} (1.23±0.04). Similarly, the COM velocity at HSR had the strongest linear relationships with ML forces and ratios at TOL. For slow walking, the vertical ground reaction force at TOL is approximately 1 for most perturbations. Consequently, the ML force at TOL (y=−0.74x−0.01, R^2=0.998) and the ML R_F at TOL (y=−0.70x−0.01, R^2=0.997) have similar relationships with the ML COM velocity at HSR. This also holds for R_D at TOL (y=−0.70x−0.01, R^2=0.994), see Fig. 7, such that the total ground reaction force in the frontal plane at TOL points approximately toward the COM for all ML perturbations. For the normal walking speed, these similarities between R_F (y=−0.97x −0.02, R^2=0.996) and R_D (−0.97x−0.02, R^2=0.997) also exist (see Fig. S3). However, the ML force shows a different relationship (y= −1.21x−0.02, R^2=0.998), as the vertical force component tends to increase with ML perturbation magnitude.

For AP perturbations, the AP distance between the COM and the leading foot at HSR shows only minor changes with AP COM velocity at HSR (slow: y=0.27x+0.43, R^2=0.281, normal: y= −0.34x+0.66, R^2=0.917; see Fig. 6, Fig. S2). As in the ML direction, the strongest linear relationships were found between the AP COM velocity at HSR and the AP distance between the COM and the COP at TOL. Again, for slow walking, the slope of the fit to this data (y=1.49x−0.31, R^2=0.982) corresponds well with ω_0^{-1}. This is less the case for the normal speed (y=0.87x−0.26, R^2=0.97). Also for AP forces and ratios at TOL, the strongest linear relationships were found with the AP COM velocity at HSR. The vertical ground reaction force at TOL tends to change with AP perturbation magnitude. Consequently, for slow walking, the relationships of both the AP force (y=−0.84x+0.19, R^2=0.988) and the AP R_F (y=−0.73x+0.17, R^2=0.983) with the AP COM velocity at HSR are less similar compared with those in the ML direction following ML perturbations. However, comparison of the fit to the AP R_F with the fit to the AP R_D (y=−0.68x+0.14, R^2=0.984; Fig. 7) suggests that the total ground reaction force in the sagittal plane points approximately toward the COM at TOL, for all perturbations. For the normal walking speed, similar comparisons can be made between the relationships of the AP COM velocity at HSR with the AP force (y=−1.19x+0.48,

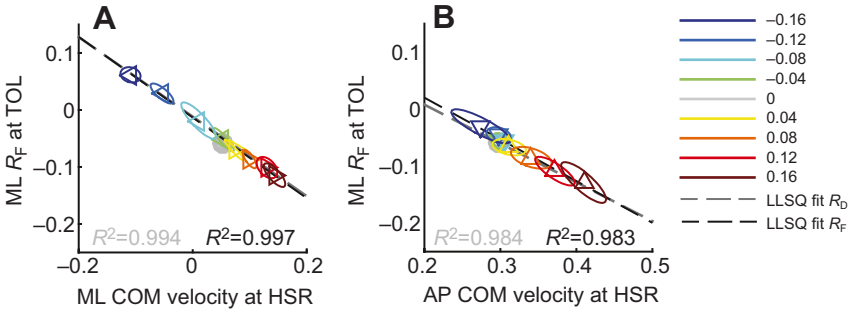

Fig. 7. Relationships between COM velocity and both force and distance ratios. (A) ML COM velocity at HSR versus ML force ratio R_F at TOL. For distance ratio R_D, only a fit to the data is shown for comparison. (B) Same as A, but in the AP direction for AP perturbations. Triangles show subject means and indicate the perturbation direction. Ellipses represent the subject standard deviation. Colors indicate the various perturbation magnitudes. Black and gray dashed lines are linear least squares fits to the data for R_F and R_D, respectively. R^2 indicates the coefficient of determination of the fits. Data shown are dimensionless and for slow walking only.

Journal of Experimental Biology (2016) 219, 1514-1523 doi:10.1242/jeb.129338

R^2=0.992), AP R_F (y=−0.74x+0.27, R^2=0.973) and AP R_D (y=−0.57x+0.17, R^2=0.973). Comparing R_F and R_D for normal walking speed (Fig. S3) suggests that the total ground reaction force in the sagittal plane at TOL tends to point above the COM for backward perturbations and below the COM for forward perturbations.

DISCUSSION

Walking human subjects were perturbed in the horizontal plane at the start of the single support phase. The distance between the COM and the COP at toe-off, as well as the horizontal ground reaction force, increased linearly with increasing horizontal COM velocity at the preceding heel strike, in both ML and AP directions. In the ML direction, foot placement is crucial to realize these COP relations given the limited possibilities for ML COP displacement within the foot. In the AP direction, other contributions such as an ankle torque are key in adjusting the COP location and the ground reaction force. Furthermore, gait phase durations varied following the perturbations, especially for ML perturbations. In the following sections, the subject responses will be discussed in order of occurrence following the perturbation.

Single support phase duration

Humans show variations in foot placement timing for the first recovery step. By controlling the swing leg, humans can choose from a tremendous amount of spatio-temporal options for foot placement. Yet all subjects show similar consistent spatial and temporal responses, suggesting a preferred recovery strategy among all possible options. This could arise from a trade-off between the energetic costs of leg swing against the expected cost for recovery after foot placement, in a way similar to that predicted for a preferred step frequency during normal walking (Kuo, 2001).

The single support duration might shorten with increasing deviation of the COM from the desired walking direction. This is mainly supported by the durations following ML perturbations. When the COM is pushed away from or over the BoS of the stance foot, the need for lateral corrections increases. This leads to a decreased single support duration. For the lower magnitude inward perturbations, the COM is laterally pushed toward but not over the stance foot. This way there is no direct need to correct for lateral imbalance, which can even increase the single support duration. After completion of any AP perturbation, the COM is still moving in the desired forward direction, possibly leading to little need to adjust the single support duration. Furthermore, effects of the AP perturbations can be partially counteracted by modulating the ankle torque of the left stance foot directly after the perturbation has been applied (not shown). A possible explanation for the increased single support duration following larger backward perturbations is that subjects wait to regain forward velocity.

In Hof et al. (2010), especially inward perturbations led to a decrease in single support duration with increasing perturbation magnitude. Although this appears to contradict the current results, Hof's perturbations were applied shortly before heel strike, mainly affecting the subsequent swing phase. Hence, temporal results for inward perturbations at HSR in Hof's work are most comparable with results for outward perturbations in this work. Significant increases in single support duration were not reported in Hof et al. (2010), most likely because of the walking speed of 1.25 m s^{-1}. In the present study, no significant increase in single support duration was found following ML perturbations during the normal walking speed.

Foot placement

The ML COM velocity at HSR has a strong predictive value for ML foot placement. This is in line with previous findings in ML foot placement (Hof et al., 2007; Wang and Srinivasan, 2014). Findings in unperturbed walking have suggested that the AP COM velocity at mid-stance also significantly contributes to predictions of the next AP foot placement location (Wang and Srinivasan, 2014). This location was expressed relative to the trailing foot, and therefore contained effects occurring between the COM and both the leading and the trailing foot. Our results suggest that the findings for AP foot placement in Wang and Srinivasan (2014) are mainly caused by changes between the COM and the trailing foot. Here, none of the AP perturbations led to a distance between the COM and the leading foot that was significantly different from the distance in unperturbed walking. Humans might choose not to adjust the AP distance between the COM and the leading foot, as increasing this distance is energetically costly. The work rate required to redirect the COM from one single support phase to the next increases with the fourth power of the step length, in both an inverted-pendulum-based collision model and human experimental data (Donelan et al., 2002). Humans might prefer a less costly recovery option, possibly provided by adjustments in ankle torque of the leading foot. Modifying the available recovery options, for example, through applying a constraint to the ankle joint of the subject, could give insight into why humans make this choice. Not adjusting the AP distance between the COM and the leading foot contradicts with COM velocity-dependent foot placement strategies that were previously used in simple inverted pendulum models (Kajita et al., 1992; Hof, 2008; Peuker et al., 2012), although these footless models have no option other than foot placement to displace the COP.

Double support phase duration

Changes in double support duration might be caused by actions both preceding and during the double support phase. First, when falling forward during the single support phase, the trailing leg extends to provide time and clearance for positioning of the leading foot (Pijnappels et al., 2005). The more extension occurs before the double support phase, the earlier the trailing leg will have to leave the floor during the double support phase, simply because it cannot extend any further. Second, the double support phase might be actively shortened or lengthened. The trailing leg cannot contribute well to horizontal forces required to slow down COM motion away from the trailing foot. A safer option could therefore be to initiate swing earlier, creating more time to prepare for the next step, which can reduce excessive velocity. Conversely, the double support phase might be lengthened when the trailing leg has to deliver additional force to regain velocity. Significant changes in the double support duration were not reported in Hof et al. (2010) following ML perturbations during walking at 1.25 m s^{-1}. In the present study, fewer changes in double support duration were observed for the normal walking speed compared with the slow walking speed following ML perturbations, although significant changes were still present.

COP location

Using simple linear relationships, the COM velocity at HSR can be used to predict the distance between the COM and the COP observed at TOL, in both ML and AP directions, for both slow and normal walking speeds. For the slow walking speed, these relationships are similar in both ML and AP directions. Although humans cannot directly sense COM velocity, underlying proprioceptive and vestibular sensing systems could be used to

make an estimate. The strong linear relationships support that such an estimate could be used to generate a proportional recovery response. However, a causal relationship between the COM velocity and the observed responses cannot be inferred from the data. Further perturbation studies, possibly combined with sensory perturbations (Kiemel et al., 2011), could be used to infer a neurological cause of these responses.

The double support phase plays an important role in establishing these relationships. They result from foot placement, COP displacements by a weight shift to the leading leg, changes in double support duration, as well as specific joint torques. Following AP perturbations, the larger range in distance between the COM and the COP at TOL compared with that between the COM and the leading foot at TOL can only be caused by effects other than foot placement, most likely an ankle torque. Hence, both passive dynamics and controlled actions prior and during the double support phase contribute to the observed linear relationships.

Most effects that play a role in establishing these relationships are not captured by simple inverted pendulum models. Yet, the relationship between the COM velocity at HSR and the COP at TOL for slow walking is in line with constant offset control (Hof, 2008). If the fit to the data has the same slope as that of the XCOM line (ω_0^{-1}), the distance between the COP and the XCOM is approximately equal for all perturbations. This distance is then given by the intercept of the fit. Similarities are further supported by applying the offsets found in the data to foot placement in the linear inverted pendulum model. This would result in model movement that is in the same direction as that of the subjects. The model would topple over the COP in the AP direction for all AP perturbations. In the ML direction, the model would return in the direction it came from following most ML perturbations. Exceptions are the larger (−0.12, −0.16) inward perturbations, for which the COP is located between the COM and the XCOM. This would make the model topple over the COP in the ML direction. Subjects likely also do this after making a cross-step, to undo the crossing of the legs in the subsequent step.

Although the model can mimic the observed relationships, it does not explain the relationships. The data violate several assumptions made in the model. Constant offset control only makes the linear inverted pendulum model converge to some stable gait as long as the swing time can be kept constant (Hof, 2008). Subjects showed adjustments to single and double support durations; hence in this scenario the linear inverted pendulum model provides no explanation for COP adjustments directly proportional to the COM velocity.

The relationships might differ for other perturbation magnitudes and types. For sufficiently large AP perturbations magnitudes, the AP COP required to satisfy the relationship is no longer obtainable without changing the foot location relative to the COM at heel strike. This could lead either to an increased distance between COM and leading foot to further expand the BoS, or to a recovery over multiple steps without adjusting this distance. Furthermore, it is unclear whether these relationships hold for other perturbation types such as tripping, which has a major effect on the body's angular momentum (Pijnappels et al., 2005).

Ground reaction force

The horizontal ground reaction force components, the distance between the COM and the COP, R_F and R_D all co-vary at TOL in both the ML and AP directions. In a similar way, co-variation between AP COP location and ground reaction force direction has previously been shown to occur throughout the unperturbed gait cycle (Maus et al., 2010; Gruben and Boehm, 2012), in which the ground reaction force appears to be directed toward a point above the COM. Although not representative of the complete gait cycle, here the ground reaction force mostly points toward the COM at TOL. The main exception is in the AP direction for the normal walking speed, where it tends to point above the COM for backward perturbations, and below the COM for forward perturbations.

Such co-variation could have advantages for balance control during walking. A change in horizontal force, for example, to modulate horizontal COM velocity, would alter the direction of the ground reaction force, and with it the angular acceleration of the body. By co-variation of either the vertical force magnitude or the COP location relative to the body, effects of a changing horizontal force on the body's angular acceleration can be prevented. Changing the vertical force would lead to fluctuations in vertical COM acceleration. Moreover, uncontrolled manifold analysis in unperturbed human walking suggests that creating a consistent vertical force is an implicit goal of walking, whereas creating a consistent AP force component is not (Toney and Chang, 2013). Simultaneous changes in horizontal force and COP location can be achieved through ankle torque modulation. It could therefore play an important role in simultaneously regulating horizontal and angular body accelerations. Previous work has suggested that an ankle torque is involved in regulating the body's angular acceleration in the sagittal plane during gait, reflected in changes in AP COP location and ground reaction force direction (Gruben and Boehm, 2014). Hence, ankle torque modulation could provide an alternative to increasing the AP distance between the COM and the leading foot during recovery.

Conclusions

The present work revealed simple linear relationships between the COM velocity at heel strike and the COP location and horizontal ground reaction forces at toe-off during perturbation recovery. These relationships are the result of passive dynamics as well as controlled actions during the single and double support phases. For slow walking, the relationship between COM velocity and COP location is comparable for both ML and AP directions, possibly indicating a similar underlying objective. However, actions taken to realize these relationships differ between the ML and AP directions. Although foot placement adjustment is crucial in the ML direction, other actions such as ankle torque modulation contribute to the relationships in the AP direction. Furthermore, changes in gait phase duration suggest that the timing of actions could play an important role in the recovery phase. A further challenge is to unravel why humans choose one recovery strategy over another, and to what extend variables such as foot placement location, COP shift and gait phase duration are actively regulated.

Many aspects that contribute to the observed relationships are often not represented in simple inverted pendulum models. Although these simple models might mimic the relationships through foot placement only, they do not necessarily provide an explanation of the observed human behavior. Using models to gain insight into why humans prefer a certain strategy requires modeling the involved degrees of freedom. Our study motivates the modeling of a double support phase, for instance, using a spring-loaded inverted pendulum (Geyer et al., 2006) that can mimic the double support through compliant legs. Our study furthermore suggests the inclusion of feet in walking models, such as in Kim and Collins (2013), where ankle control was used to stabilize a walking model. Such extended models are required to investigate the underlying costs and constraints that determine the balance strategies employed

Journal of Experimental Biology

by humans during walking. Further mining of human data for simplified expressions of balance in walking can support making such models more human-like.

Acknowledgements
The authors thank D. W. Boere for her assistance in data collection.

Competing interests
The authors declare no competing or financial interests.

Author contributions
M.V.: study design, data collection and analysis, and manuscript preparation and revision. E.H.F.v.A.: study design, data analysis and manuscript revision. H.v.d.K.: study design, data analysis and manuscript revision.

Funding
This work was supported by the BALANCE (Balance Augmentation in Locomotion, through Anticipative, Natural and Cooperative control of Exoskeletons) project, partially funded under grant number 601003 of the Seventh Framework Programme (FP7) of the European Commission (Information and Communication Technologies, ICT-2011.2.1). The funding parties had no role in study design, data collection and analysis, decision to publish, or preparation of the manuscript.

Supplementary information
Supplementary information available online at
http://jeb.biologists.org/lookup/suppl/doi:10.1242/jeb.129338/-/DC1

References

Cappozzo, A., Catani, F., Della Croce, U. and Leardini, A. (1995). Position and orientation in space of bones during movement: anatomical frame definition and determination. *Clin. Biomech.* **10**, 171-178.
Donelan, J. M., Kram, R. and Kuo, A. D. (2002). Mechanical work for step-to-step transitions is a major determinant of the metabolic cost of human walking. *J. Exp. Biol.* **205**, 3717-3727.
Dumas, R., Chèze, L. Verriest, J.-P. (2007). Adjustments to McConville et al. and Young et al. body segment inertial parameters. *J. Biomech.* **40**, 543-553.
Garcia, M., Chatterjee, A., Ruina, A. and Coleman, M. (1998). The simplest walking model: stability, complexity, and scaling. *J. Biomech. Eng.* **120**, 281-288.
Geyer, H., Seyfarth, A. and Blickhan, R. (2006). Compliant leg behaviour explains basic dynamics of walking and running. *Proc. R. Soc. B Biol. Sci.* **273**, 2861-2867.
Gruben, K. G. and Boehm, W. L. (2012). Force direction pattern stabilizes sagittal plane mechanics of human walking. *Hum. Mov. Sci.* **31**, 649-659.
Gruben, K. G. and Boehm, W. L. (2014). Ankle torque control that shifts the center of pressure from heel to toe contributes non-zero sagittal plane angular momentum during human walking. *J. Biomech.* **47**, 1389-1394.
Hodgins, J. K. and Raibert, M. (1991). Adjusting step length for rough terrain locomotion. *IEEE Trans. Robot. Autom.* **7**, 289-298.
Hof, A. L. (1996). Scaling gait data to body size. *Gait Posture* **4**, 222-223.
Hof, A. L. (2008). The 'extrapolated center of mass' concept suggests a simple control of balance in walking. *Hum. Mov. Sci.* **27**, 112-125.
Hof, A. L., Gazendam, M. G. J. and Sinke, W. E. (2005). The condition for dynamic stability. *J. Biomech.* **38**, 1-8.
Hof, A. L., van Bockel, R. M., Schoppen, T. and Postema, K. (2007). Control of lateral balance in walking. Experimental findings in normal subjects and above-knee amputees. *Gait Posture* **25**, 250-258.
Hof, A. L., Vermerris, S. M. and Gjaltema, W. A. (2010). Balance responses to lateral perturbations in human treadmill walking. *J. Exp. Biol.* **213**, 2655-2664.
Jian, Y., Winter, D. A., Ishac, M. G. and Gilchrist, L. (1993). Trajectory of the body COG and COP during initiation and termination of gait. *Gait Posture* **1**, 9-22.
Kajita, S. and Tani, K. (1991). Study of dynamic biped locomotion on rugged terrain: derivation and application of the linear inverted pendulum mode. In *Proceedings of the 1991 IEEE Conference on Robotics and Automation, Vol.* **2**, pp. 1405-1411. Sacramento, CA: IEEE.
Kajita, S., Yamaura, T. and Kobayashi, A. (1992). Dynamic walking control of a biped robot along a potential energy conserving orbit. *IEEE Trans. Robot. Autom.* **8**, 431-438.
Kiemel, T., Zhang, Y. and Jeka, J. J. (2011). Identification of neural feedback for upright stance in humans: Stabilization rather than sway minimization. *J. Neurosci.* **31**, 15144-15153.
Kim, M. and Collins, S. H. (2013). Stabilization of a three-dimensional limit cycle walking model through step-to-step ankle control. In *2013 IEEE International Conference on Rehabilitation Robotics (ICORR)*, pp. 1-6. Seattle, WA: IEEE.
Kuo, A. D. (2001). A simple model of bipedal walking predicts the preferred speed–step length relationship. *J. Biomech. Eng.* **123**, 264-269.
MacKinnon, C. D. and Winter, D. A. (1993). Control of whole body balance in the frontal plane during human walking. *J. Biomech.* **26**, 633-644.
Maus, H.-M. and Seyfarth, A. (2014). Walking in circles: a modelling approach. *J. R. Soc. Interface* **11**, 20140594.
Maus, H. M., Lipfert, S., Gross, M., Rummel, J. and Seyfarth, A. (2010). Upright human gait did not provide a major mechanical challenge for our ancestors. *Nat. Commun.* **1**, 70.
Patla, A. E. (2003). Strategies for dynamic stability during adaptive human locomotion. *IEEE Eng. Med. Biol. Mag.* **22**, 48-52.
Peuker, F., Maufroy, C. and Seyfarth, A. (2012). Leg-adjustment strategies for stable running in three dimensions. *Bioinspir. Biomim.* **7**, 036002.
Pijnappels, M., Bobbert, M. F. and van Dieën, J. H. (2005). How early reactions in the support limb contribute to balance recovery after tripping. *J. Biomech.* **38**, 627-634.
Pratt, J., Carff, J., Drakunov, S. and Goswami, A. (2006). Capture point: a step toward humanoid push recovery. In *Proceedings of the Sixth IEEE-RAS International Conference on Humanoid Robots*, pp. 200-207. Genova, Italy: IEEE.
Robinovitch, S. N., Feldman, F., Yang, Y., Schonnop, R., Leung, P. M., Sarraf, T., Sims-Gould, J. and Loughin, M. (2013). Video capture of the circumstances of falls in elderly people residing in long-term care: an observational study. *Lancet* **381**, 47-54.
Söderkvist, I. and Wedin, P.-Å. (1993). Determining the movements of the skeleton using well-configured markers. *J. Biomech.* **26**, 1473-1477.
Toney, M. E. and Chang, Y.-H. (2013). Humans robustly adhere to dynamic walking principles by harnessing motor abundance to control forces. *Exp. Brain Res.* **231**, 433-443.
Townsend, M. A. (1985). Biped gait stabilization via foot placement. *J. Biomech.* **18**, 21-38.
Wang, Y. and Srinivasan, M. (2014). Stepping in the direction of the fall: the next foot placement can be predicted from current upper body state in steady-state walking. *Biol. Lett.* **10**, 20140405.
Winter, D. A. (1995). Human balance and posture control during standing and walking. *Gait Posture* **3**, 193-214.
Zeni, J., Jr, Richards, J. and Higginson, J. (2008). Two simple methods for determining gait events during treadmill and overground walking using kinematic data. *Gait Posture* **27**, 710-714.